

# Constraining neutron superfluidity with $r$ -mode physics

Elena M. Kantor, Mikhail E. Gusakov, and Vasilii A. Dommes  
*Ioffe Institute, Polytekhnicheskaya 26, 194021 St.-Petersburg, Russia*

We constrain the parameters of neutron superfluidity in the cores of neutron stars making use of the recently proposed effect of resonance stabilization of  $r$ -modes. To this end, we, for the first time, calculate the finite-temperature  $r$ -mode spectra for realistic models of rotating superfluid neutron stars, accounting for both muons and neutron-proton entrainment in their interiors. We find that the ordinary (normal)  $r$ -mode exhibits avoided crossings with superfluid  $r$ -modes at certain stellar temperatures and spin frequencies. Near the avoided crossings, the normal  $r$ -mode dissipates strongly, which leads to substantial suppression of the  $r$ -mode instability there. The extreme sensitivity of the positions of avoided crossings to the neutron superfluidity model allows us to constrain the latter by confronting the calculated spectra with observations of rapidly rotating neutron stars in low-mass X-ray binaries.

*Introduction.*— Since 1998, when it was discovered [1, 2], the  $r$ -mode instability has been a problem for neutron star (NS) physics [3–10].  $R$ -modes are predominantly toroidal oscillations (i.e., oscillations with a divergenceless velocity field and a suppressed radial component of the velocity [11]) of rotating stars restored by the Coriolis force. Their close relatives are Rossby waves on Earth. Neglecting dissipation, they are unstable with respect to gravitational radiation at any spin frequency  $\nu$  of an NS. Dissipation, however, suppresses this instability to some extent. Cold and hot NSs are effectively stabilized by shear and bulk viscosities, respectively [11], but the stabilizing mechanism for rapidly rotating NSs of intermediate internal temperatures,  $T^\infty \sim 10^8$  K (redshifted, as seen by a distant observer), is not so obvious. Seemingly, we should not observe NSs in the region of  $\nu$  and  $T^\infty$  where the  $r$ -mode instability is not suppressed by dissipation (the “instability window”), since, as the theory predicts, the excited  $r$ -mode rapidly spins the star down by means of gravitational radiation so that the probability of finding an NS in this region is negligible [12–14]. However, the observations show [13, 15, 16] that numerous NSs fall well inside the classical (i.e., calculated under minimal assumptions) instability window. These stars belong to low-mass X-ray binaries (LMXBs), where they are heated and spun up by accretion from the low-mass companion. A series of proposals have been suggested to solve the puzzle of NSs in the instability window (see [14, 17] for the reviews). Most of them either involve exotic physics (e.g., a quark or hyperon composition of the NS core) or make some model-dependent assumptions about the mechanism of the nonlinear saturation of  $r$ -modes [14]. One of the proposals is the resonance stabilization of  $r$ -mode by superfluid (SF) modes [9, 13, 18]. The latter does not require any exotic physics and adopts standard assumptions about the properties of NS matter, the same as in the minimal cooling scenario [19, 20].

*Resonance  $r$ -mode stabilization scenario.*— We consider the  $npe\mu$ -composition of an NS core: neutrons ( $n$ ), protons ( $p$ ), electrons ( $e$ ), and muons ( $\mu$ ), and account for a

possible nucleon SF [21, 22]. SF NSs can support several independent velocity fields: the velocity of SF neutrons and the velocity of the remaining components [23, 24] (the proton SF velocity is not independent since protons are coupled with electrons and muons by electromagnetic forces). As a result, new SF modes appear in the NS oscillation spectrum in addition to ordinary (normal) modes of non-SF NSs [25–27]. In contrast to the normal modes, SF modes strongly depend on  $T^\infty$  because of temperature dependence of neutron SF density [23, 28–33] (more precisely, of the entrainment matrix  $Y_{ik}$ ; see below). Consequently, normal and SF modes exhibit avoided crossings at a certain (resonance)  $T^\infty$ , where the eigenfrequency of the SF mode approaches that of the normal mode. SF modes dissipate efficiently due to powerful mutual-friction mechanism [34], which tends to equalize the velocities of normal and SF components, while for normal  $r$ -modes mutual friction is, generally, not effective. However, at resonance  $T^\infty$ , the normal and SF modes interact strongly, the eigenfunction of the SF mode admixes to the eigenfunction of the normal mode, and the latter experiences resonance stabilization by mutual friction at these  $T^\infty$  [9, 13]. The scenario of [9, 13] uses this property to stabilize normal  $r$ -modes for NSs observed in the classical instability window. According to [9, 13], NSs in that window should have  $\nu$  and  $T^\infty$  corresponding to resonances between the SF and normal modes.

Initially, this scenario was proposed as a purely phenomenological one. In this Letter, we develop it into a quantitative theory. To this end, we calculate temperature-dependent  $r$ -mode spectra of rotating SF NSs for realistic three-layer stellar configurations, consisting of a barotropic crust treated as a single fluid, an  $npe$  outer core and an  $npe\mu$  inner core. Calculations are performed adopting up-to-date microphysics input, including nonzero entrainment between neutrons and protons, realistic equations of state (EOSs), and the parameters of a nucleon SF. Confronting the calculated spectra with the available observations of NSs in LMXBs allows us to put constraints on the neutron SF critical temperature profile in the NS core.

*Oscillation equations.*— We consider nondissipative oscillations of a slowly rotating (spin frequency  $\Omega = 2\pi\nu$ ) NS. We adopt the Cowling approximation (i.e., neglect metric perturbations [35]) and work in the Newtonian framework. The linearized equations governing small oscillations of SF NSs in the frame rotating with the star are as follows [36]:

(i) Euler equation

$$\frac{\partial \mathbf{v}_b}{\partial t} + 2\boldsymbol{\Omega} \times \mathbf{v}_b = -\delta \left( \frac{\nabla P}{w} \right) = \frac{\delta w}{w^2} \nabla P - \frac{\nabla \delta P}{w}, \quad (1)$$

where  $w = (P + \epsilon)/c^2$ ,  $P$  is the pressure,  $\epsilon$  is the energy density (including the rest mass energy density),  $c$  is the speed of light, and  $t$  is time. Here and hereafter,  $\delta$  stands for the Eulerian perturbation of the corresponding thermodynamic parameter. The small (first order) perturbation of the velocity of baryons is  $\mathbf{v}_b \equiv \mathbf{j}_b/n_b$ , where  $n_b \equiv n_n + n_p$ ,  $\mathbf{j}_b \equiv \mathbf{j}_n + \mathbf{j}_p$ , and  $n_i, \mathbf{j}_i$  ( $i = n, p$ ) are the particle number density and current density, respectively.

(ii) Continuity equations for baryons and leptons ( $l = e, \mu$ )

$$\frac{\partial \delta n_b}{\partial t} + \text{div}(n_b \mathbf{v}_b) = 0, \quad \frac{\partial \delta n_l}{\partial t} + \text{div}(n_l \mathbf{v}) = 0, \quad (2)$$

where  $\mathbf{v}$  is the small (first order) perturbation of the velocity of normal liquid component (leptons and baryon thermal excitations).

(iii) The “superfluid” equation [a combination of the Euler equation for the SF neutron liquid component and Eq. (1)]

$$-h \frac{\partial \mathbf{v}_\Delta}{\partial t} - 2h_1 \boldsymbol{\Omega} \times \mathbf{v}_\Delta = c^2 n_e \nabla \Delta \mu_e + c^2 n_\mu \nabla \Delta \mu_\mu, \quad (3)$$

where  $\mathbf{v}_\Delta \equiv \mathbf{v}_b - \mathbf{v}$ ;  $\Delta \mu_l \equiv \mu_n - \mu_p - \mu_l$  is the chemical potential imbalance; in thermodynamic equilibrium  $\Delta \mu_l = 0$  [37]. Further,

$$h = n_b \mu_n \left[ \frac{n_b Y_{pp}}{\mu_n (Y_{nn} Y_{pp} - Y_{np}^2)} - 1 \right], \quad (4)$$

$$h_1 = n_b \mu_n \left( \frac{n_b}{Y_{nn} \mu_n + Y_{np} \mu_p} - 1 \right), \quad (5)$$

where  $Y_{ik}$  ( $i, k = n, p$ ) is the temperature-dependent entrainment matrix [24, 28, 33, 38, 39], which is a generalization of the concept of SF density (e.g., [23]) to the case of SF mixtures. The off-diagonal elements  $Y_{np} = Y_{pn}$  of this matrix describe the “entrainment effect”, i.e., the mass transfer of one SF particle species by the SF motion of another species. Typically, this effect is rather weak (in other words,  $Y_{np}$  is sufficiently small; see, e.g., [40]), so that  $h_1 \approx h$ . Eqs. (1)–(5) should be supplemented with this relation:  $\delta n_\alpha = \frac{\partial n_\alpha}{\partial P} \delta P + \frac{\partial n_\alpha}{\partial \Delta \mu_e} \Delta \mu_e + \frac{\partial n_\alpha}{\partial \Delta \mu_\mu} \Delta \mu_\mu$ ,  $\alpha = n, p, e, \mu$ .

Now, consider NS perturbations that depend on time  $t$  as  $e^{i\sigma t}$  in the corotating frame. Then, following the same

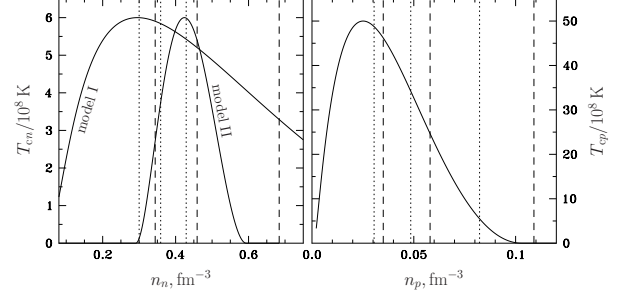


FIG. 1: Profiles  $T_{cn}(n_n)$  and  $T_{cp}(n_p)$ , respectively, for the neutron SF models I and II (left panel) and the proton SF model (right panel). Vertical lines (dashes for APR EOS, dots for BSk24 EOS) show the central number densities of NSs with, from left to right,  $M = 1.0M_\odot$ ,  $1.4M_\odot$ , and  $1.8M_\odot$ .

procedure as for non-SF stars (e.g., [41]), we expand all the unknown functions into spherical harmonics  $Y_{lm}$  with fixed  $m$ . In addition, we also expand all the quantities in a power series in small parameter  $\Omega$  (here and in what follows we normalize  $\Omega$  and  $\sigma$  to the Kepler frequency). We are interested in the oscillations, that are absent in nonrotating stars, i.e., that have the eigenfrequencies  $\sigma$  vanishing at  $\Omega \rightarrow 0$ . In this case,  $\sigma$  can be represented as follows (e.g., [41–43]):  $\sigma = \sigma_0 \Omega + O(\Omega^3)$ . When considering NSs with SF  $npe\mu$  cores, we found in [36] that, for vanishing entrainment [when  $Y_{np} = Y_{pn} = 0$ , i.e.,  $h_1 = h$ ; see Eqs. (4), (5)], purely toroidal modes (in the lowest order in  $\Omega$ ) are only possible if  $l = m$ . For a given  $m$  there exist one normal  $r$ -mode and an infinite set of SF  $r$ -modes, all having the same  $\sigma_0$ :  $\sigma_0 = 2/(m+1)$  [36, 44–46].

When neutron and proton SFs coexist somewhere in an NS, entrainment between neutrons and protons, although weak, plays an important role, because it affects the position of avoided crossings as discussed below. Assuming that the entrainment effect is small, we develop a perturbation theory in the parameter  $\Delta h \equiv h/h_1 - 1 \ll 1$  [40]. We account for both the corrections due to entrainment and next-to-leading order corrections in  $\Omega$  in oscillation equations, and treat them simultaneously, expanding the oscillation frequency as

$$\sigma = (\sigma_0 + \sigma_1)\Omega, \quad (6)$$

where  $\sigma_1$  corresponds to the next-to-leading-order correction in  $\Omega$  and  $\Delta h$ .

*Physics input.*— We consider two realistic EOSs. The first one (denoted as APR EOS) uses the parametrization [47] of Akmal-Pandharipande-Ravenhall (APR) EOS from [48], and adopts  $Y_{ik}$  from [30]. The second one (BSk24 EOS) is obtained from the BSk24 energy-density functional [49, 50]; the same functional is used to calculate  $Y_{ik}$  in a self-consistent manner [31, 33, 38, 39]. For

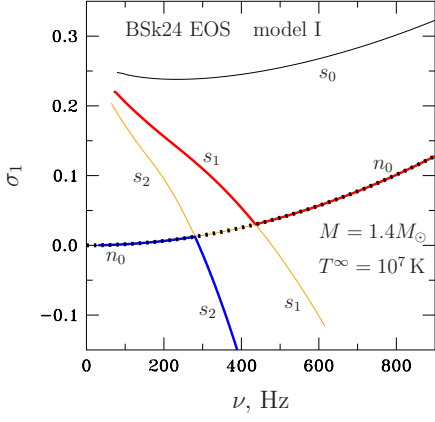


FIG. 2:  $\sigma_1$  versus  $\nu$  for normal  $r$ -mode ( $n_0$ ) and first three SF  $r$ -modes ( $s_0, s_1, s_2$ ).

each of these EOSs, we consider one model of a proton SF and two models, I and II, of neutron SF, that differ by the width of the density-dependent profile of the (local) neutron critical temperature,  $T_{cn}(n_n)$  (Fig. 1). The adopted models have maximum critical temperatures that do not contradict the existing data on cooling NSs [19, 20, 51–56] and the microscopic calculations [21, 22, 57–60]. The wider profile of  $T_{cn}$  (model I), which extends to lower densities, is favored more by the microscopic theory. In turn, the narrower profiles (similar to model II) have been used in a number of works (e.g., [20, 51, 52, 54]) to successfully explain the thermal properties of isolated NSs within the minimal cooling scenario [19, 20].

*Results.*— All results obtained below are for  $l = m = 2$   $r$ -modes, since the  $l = m = 2$  nodeless normal  $r$ -mode is believed to be the most unstable one [11]. Figure 2 shows how  $\sigma_1$  depends on  $\nu$  for an NS with the mass  $M = 1.4M_\odot$  and  $T^\infty = 10^7$  K, assuming BSk24 EOS, and SF model I. In this case the  $r$ -mode spectrum consists of one normal nodeless  $r$ -mode  $n_0$ , one SF nodeless  $r$ -mode  $s_0$ , and an infinite set of SF modes with nodes (only the two first overtones,  $s_1$  and  $s_2$ , are plotted in Fig. 2). Different modes are shown by different width lines. Avoided crossings  $n_0, s_1$  and  $n_0, s_2$  are clearly visible where the modes change their behavior from normal ( $n_0$ ) to SF-like ( $s_1$  or  $s_2$ ) and vice versa. Dots show the normal  $r$ -mode (at different temperatures different modes behave as the normal one).

Since  $Y_{ik}$  (and hence parameters  $h$  and  $h_1$ , entering the oscillation equations) depends on  $T^\infty$ , the spin frequencies  $\nu_{n_0, s_\alpha}$ , at which avoided crossings  $n_0, s_\alpha$  occur, will also be temperature dependent ( $\alpha = 0, 1, 2$ , and so on). Fig. 3 shows the curves  $\nu_{n_0, s_\alpha}(T^\infty)$  plotted for NSs with different masses, assuming APR and BSk24 EOSs and models I and II of the neutron SF. The gray area is a classical stability region determined solely by the shear viscosity. It is calculated for an NS with the mass

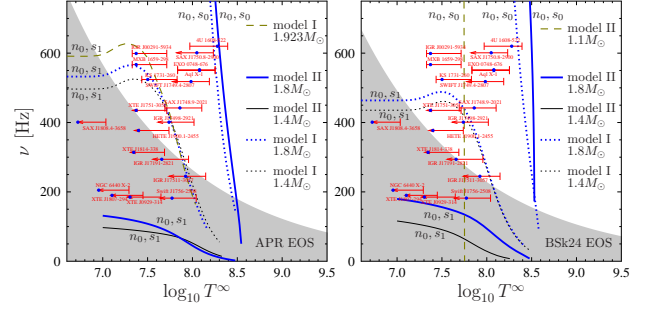


FIG. 3: The curves  $\nu_{n_0, s_0}(T^\infty)$  (marked  $n_0, s_0$ ) and  $\nu_{n_0, s_1}(T^\infty)$  (marked  $n_0, s_1$ ), showing  $\nu$  and  $T^\infty$  at which normal  $r$ -mode exhibits avoided crossings with the  $s_0$  and  $s_1$  SF  $r$ -modes. Left panel shows results for APR EOS, right panel – for BSk24 EOS. Thick and thin curves are plotted for NSs with  $M = 1.8M_\odot$  and  $1.4M_\odot$ , respectively. Dots correspond to model I, solid lines – to model II. Dashes in the left panel show  $\nu_{n_0, s_1}(T^\infty)$  for the maximum-mass configuration ( $M = 1.923M_\odot$ ) and model I. Dashes in the right panel show  $\nu_{n_0, s_0}(T^\infty)$  for  $M = 1.1M_\odot$  and model II.

$M = 1.8M_\odot$ . The points correspond to available observational data on NSs in LMXBs [9, 61]. The error bars describe uncertainties in the stellar envelope composition [9]. As one can see, many sources lie in the classical instability window (white region in Fig. 3), which imposes a problem for a classical  $r$ -mode scenario. According to our proposal [9, 13], the  $r$ -mode instability for these sources is suppressed because they are all located near the curves  $\nu_{n_0, s_\alpha}(T^\infty)$ , where  $r$ -mode dissipation is enhanced by resonance interaction with one of the SF modes.

Generally (at not too high  $T^\infty$ ; see below) avoided crossing  $n_0, s_0$  takes place at an unrealistically high  $\nu$ . Only when  $T^\infty$  approaches  $T_{cn \max}^\infty$  (the maximum of the redshifted  $T_{cn}$  in the region of the core, where neutron and proton SFs co-exist),  $\nu_{n_0, s_0}$  does start to decrease rapidly with increasing  $T^\infty$  and vanishes at  $T^\infty = T_{cn \max}^\infty$ . While  $T_{cn \max} = 6 \times 10^8$  K for our SF models,  $T_{cn \max}^\infty$  depends on the NS mass and EOS through the redshift parameter and varies in the range  $T_{cn \max}^\infty \sim (2.5-4) \times 10^8$  K. As a result, we have an almost vertical drop of  $\nu_{n_0, s_0}$  at  $T^\infty \sim (2-4) \times 10^8$  K (see Fig. 3). (We do not plot  $\nu_{n_0, s_0}$  for  $M = 1.4M_\odot$  NS because it is similar to the  $M = 1.8M_\odot$  case.) The exception is low-mass configurations for the SF model II (dashes on the right panel of Fig. 3 corresponding to  $M = 1.1M_\odot$ ), for which  $T_{cn \max}^\infty$  is small (see Fig. 1).

Avoided crossing  $n_0, s_1$  lies at a lower  $\nu$  than  $n_0, s_0$ . For model I  $\nu_{n_0, s_1}$  passes through the sources in the instability window and thus explains them. At the same time, for model II, the corresponding  $\nu_{n_0, s_1}$  is much lower. This happens because in this model  $T_{cn}$  drops sharply in the outer core, shrinking the SF region even at low  $T^\infty$ . As we checked for various SF models, such shrinking of

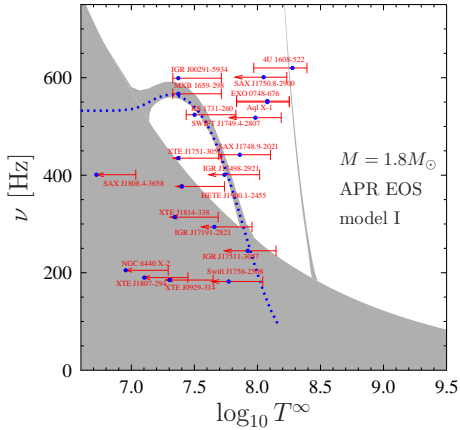


FIG. 4: Instability window for  $l = m = 2$  normal  $r$ -mode calculated for  $M = 1.8M_{\odot}$  NS with APR EOS and SF model I. In the filled region, the NS is stable. Dotted line shows  $\nu_{n_0,s_1}(T^{\infty})$  (the same line as in Fig. 3). We do not plot the curve  $\nu_{n_0,s_0}(T^{\infty})$  here, but it follows the corresponding stability peak.

the SF region in the outer core leads to a dramatic decrease of  $\nu_{n_0,s_1}$  at a given  $T^{\infty}$ . An analogous shrinking of the SF region due to a drop of  $T_{cn}$  at its higher-density slope (in the stellar center) also leads to a  $\nu_{n_0,s_1}$  decrease; this decrease, however, is not so pronounced.

Enhanced dissipation of the normal  $r$ -mode near avoided crossings stabilizes the mode, and thus should affect the classical instability window. This is illustrated in Fig. 4, which shows the instability window for an NS with  $M = 1.8M_{\odot}$ , assuming APR EOS and SF model I. To calculate the window, we accounted for shear viscosity and mutual friction dissipation, as described in [36]. One notices the appearance of “stability strips” along the curves  $\nu_{n_0,s_{\alpha}}(T^{\infty})$  (they were termed stability peaks in the initial scenario of [9, 13]). All the observed sources should be located in the stability region, which, however, varies with the stellar mass.

*Discussion.*— We show that resonance stabilization of normal  $r$ -mode indeed occurs in the range of parameters relevant to NSs, falling within the classical instability window. In that sense, our calculations confirm the phenomenological scenario [9, 13] and put it on a solid ground. Note that our results imply that stability peaks are not vertical (see Fig. 4), as the simple model [9, 13] predicted. Nevertheless, an NS in the course of its evolution in LMXB will spend most of the time climbing up the left edge of the “peak”, as demonstrated in [9, 13].

The presented calculations allow us to constrain models of a neutron SF. (Note that the proton SF only weakly affects the oscillation modes [24, 27, 62] and thus cannot be constrained by observations.) Namely, hottest rapidly rotating sources can be stabilized by resonance interaction of normal  $r$ -mode  $n_0$  with the main harmonic  $s_0$  of

the SF  $r$ -mode. Since the curve  $\nu_{n_0,s_0}(T^{\infty})$  for this resonance falls almost vertically to zero at  $T^{\infty} = T_{cn}^{\infty}$ , we can constrain the value of  $T_{cn}^{\infty}$ : it should be  $T_{cn}^{\infty} \sim (3 - 6) \times 10^8$  K. The  $T_{cn}$  profiles adopted in this paper correspond to the upper limit of this range, and Fig. 3 implies that higher values of  $T_{cn}^{\infty}$  are not favorable. On the other hand, changing  $T_{cn}^{\infty}$  to the value  $3 \times 10^8$  K shifts  $\nu_{n_0,s_0}(T^{\infty})$  to the left end of the error bar for the hottest source 4U 1608-522, so that further decrease of  $T_{cn}^{\infty}$  complicates interpretation of this source. We should stress that real maximum of  $T_{cn}$  can be larger than  $T_{cn}^{\infty}$  (the maximum of  $T_{cn}$  in the region of the core, where neutron and proton SFs co-exist). Thus, our estimate  $(3 - 6) \times 10^8$  K is the *lower limit* for the maximum value of  $T_{cn}$ . This estimate is in line with the constraints following from observations of cooling NSs [19, 20, 51–56] and it does not contradict microscopic calculations [21, 22, 57–60]. NSs in the instability window that are not too hot may be stabilized by the resonance  $n_0, s_1$  for some NS models, but only if  $T_{cn}$  profile is sufficiently wide, which ensures that the neutrons are superfluid in a significant part of the NS core at temperatures relevant to NSs in LMXBs. An example of a wide profile is our model I. Otherwise, if  $T_{cn}$  profile is narrow, like in our model II, explanation of moderately heated sources is problematic. In such cases, they may be stabilized only by the resonance with the main harmonic of the SF  $r$ -mode if we assume low masses for these sources (see the dashes in the right panel of Fig. 3). But this alternative is questionable since NSs in LMXBs are believed to have high masses [63, 64].

An analysis of Fig. 3 shows that the interpretation of the existing sources depends not only on the SF model but also on the EOS. While both EOSs employed in this Letter are considered to be realistic, they lead to substantially different (by tens of percent) curves  $\nu_{n_0,s_{\alpha}}(T^{\infty})$  (compare the two panels in Fig. 3). This occurrence opens up an intriguing possibility of using observations of NSs in LMXBs not only for constraining SF models but also for constraining EOS of superdense matter, which is still poorly known at high densities [65, 66]. To reach this goal, more accurate calculations of  $r$ -mode spectrum are required, accounting for General Relativity effects, gravitational field perturbations, and higher-order terms in the expansion (6).

In this Letter we focus on the resonance stabilization scenario, which we consider as a minimal extension of the classical scenario, capable of explaining observations. However, other mechanisms of  $r$ -mode stabilization should also operate in NSs, first of all, Ekman layer dissipation [67–69], as well as bulk viscosity in hyperon/quark matter [70–72], enhanced mutual friction dissipation [73] etc. Real instability window may be a result of interplay of various stabilization mechanisms.

We thank A.I. Chugunov for discussion. MG acknowledges the financial support from the Foundation for the



Advancement of Theoretical Physics and Mathematics BASIS (Grant No. 17-12-204-1) and from RFBR (Grant No. 18-32-20170). EK and VD thank Russian Science Foundation (Grant No. 19-12-00133) for the financial support of spectra calculations.

- 
- [1] N. Andersson, *Astrophys. J.* **502**, 708 (1998), arXiv:gr-qc/9706075.
- [2] J. L. Friedman and S. M. Morsink, *Astrophys. J.* **502**, 714 (1998), arXiv:gr-qc/9706073.
- [3] L. Lindblom, B. J. Owen, and S. M. Morsink, *Phys. Rev. Lett.* **80**, 4843 (1998), gr-qc/9803053.
- [4] L. Lindblom, J. E. Tohline, and M. Vallisneri, *Phys. Rev. Lett.* **86**, 1152 (2001), astro-ph/0010653.
- [5] A. Reisenegger and A. Bonačić, *Phys. Rev. Lett.* **91**, 201103 (2003), astro-ph/0303375.
- [6] M. Mannarelli, C. Manuel, and B. A. Sa'D, *Phys. Rev. Lett.* **101**, 241101 (2008), 0807.3264.
- [7] W. C. G. Ho, N. Andersson, and B. Haskell, *Physical Review Letters* **107**, 101101 (2011), 1107.5064.
- [8] M. G. Alford and K. Schwenzer, *Phys. Rev. Lett.* **113**, 251102 (2014), 1310.3524.
- [9] M. E. Gusakov, A. I. Chugunov, and E. M. Kantor, *Physical Review Letters* **112**, 151101 (2014), 1310.8103.
- [10] B. Haskell and A. Patruno, *Phys. Rev. Lett.* **119**, 161103 (2017), 1703.08374.
- [11] N. Andersson and K. D. Kokkotas, *International Journal of Modern Physics D* **10**, 381 (2001), gr-qc/0010102.
- [12] Y. Levin, *Astrophys. J.* **517**, 328 (1999), astro-ph/9810471.
- [13] M. E. Gusakov, A. I. Chugunov, and E. M. Kantor, *Phys. Rev. D* **90**, 063001 (2014), 1305.3825.
- [14] B. Haskell, *International Journal of Modern Physics E* **24**, 1541007 (2015), 1509.04370.
- [15] B. Haskell, N. Degenaar, and W. C. G. Ho, *Mon. Not. R. Astron. Soc.* **424**, 93 (2012), 1201.2101.
- [16] A. I. Chugunov, M. E. Gusakov, and E. M. Kantor, *Mon. Not. R. Astron. Soc.* **468**, 291 (2017), 1610.06380.
- [17] K. Glampedakis and L. Gualtieri, *Gravitational Waves from Single Neutron Stars: An Advanced Detector Era Survey* (2018), vol. 457 of *Astrophysics and Space Science Library*, p. 673.
- [18] A. I. Chugunov, M. E. Gusakov, and E. M. Kantor, *Mon. Not. R. Astron. Soc.* **445**, 385 (2014), 1408.6770.
- [19] D. Page, J. M. Lattimer, M. Prakash, and A. W. Steiner, *Astrophys. J. Suppl. Ser.* **155**, 623 (2004), astro-ph/0403657.
- [20] M. E. Gusakov, A. D. Kaminker, D. G. Yakovlev, and O. Y. Gnedin, *Astron. Astrophys.* **423**, 1063 (2004), astro-ph/0404002.
- [21] D. G. Yakovlev, K. P. Levenfish, and Y. A. Shibano, *Sov. Phys.—Usp.* **42**, 737 (1999).
- [22] U. Lombardo and H.-J. Schulze, in *Physics of Neutron Star Interiors*, edited by D. Blaschke, N. K. Glendenning, and A. Sedrakian (2001), vol. 578 of *Lecture Notes in Physics*, Berlin Springer Verlag, p. 30.
- [23] I. M. Khalatnikov, *An Introduction to the Theory of Superfluidity* (Addison-Wesley, New York, 1989).
- [24] M. E. Gusakov and N. Andersson, *Mon. Not. R. Astron. Soc.* **372**, 1776 (2006).
- [25] L. Lindblom and G. Mendell, *Astrophys. J.* **421**, 689 (1994).
- [26] U. Lee, *Astron. Astrophys.* **303**, 515 (1995).
- [27] L. Gualtieri, E. M. Kantor, M. E. Gusakov, and A. I. Chugunov, *Phys. Rev. D* **90**, 024010 (2014), 1404.7512.
- [28] A. F. Andreev and E. P. Bashkin, *Soviet Journal of Experimental and Theoretical Physics* **42**, 164 (1976).
- [29] M. Borumand, R. Joynt, and W. Kluźniak, *Phys. Rev. C* **54**, 2745 (1996).
- [30] M. E. Gusakov and P. Haensel, *Nuclear Physics A* **761**, 333 (2005), astro-ph/0508104.
- [31] N. Chamel and P. Haensel, *Phys. Rev. C* **73**, 045802 (2006), nucl-th/0603018.
- [32] N. Chamel, *Mon. Not. R. Astron. Soc.* **388**, 737 (2008), 0805.1007.
- [33] M. E. Gusakov, E. M. Kantor, and P. Haensel, *Phys. Rev. C* **80**, 015803 (2009).
- [34] M. A. Alpar, S. A. Langer, and J. A. Sauls, *Astrophys. J.* **282**, 533 (1984).
- [35] T. G. Cowling, *Mon. Not. R. Astron. Soc.* **101**, 367 (1941).
- [36] E. M. Kantor and M. E. Gusakov, *Mon. Not. R. Astron. Soc.* **469**, 3928 (2017), 1705.06027.
- [37] P. Haensel, A. Y. Potekhin, and D. G. Yakovlev, eds., *Neutron Stars 1 : Equation of State and Structure*, vol. 326 of *Astrophysics and Space Science Library* (2007).
- [38] M. E. Gusakov, E. M. Kantor, and P. Haensel, *Phys. Rev. C* **79**, 055806 (2009).
- [39] M. E. Gusakov, P. Haensel, and E. M. Kantor, *Mon. Not. R. Astron. Soc.* **439**, 318 (2014), 1401.2827.
- [40] V. A. Dommles, E. M. Kantor, and M. E. Gusakov, *Mon. Not. R. Astron. Soc.* **482**, 2573 (2019), 1810.08005.
- [41] K. H. Lockitch and J. L. Friedman, *Astrophys. J.* **521**, 764 (1999), gr-qc/9812019.
- [42] H. Saio, *Astrophys. J.* **256**, 717 (1982).
- [43] J. Provost, G. Berthomieu, and A. Rocca, *Astron. Astrophys.* **94**, 126 (1981).
- [44] N. Andersson and G. L. Comer, *Mon. Not. R. Astron. Soc.* **328**, 1129 (2001), astro-ph/0101193.
- [45] U. Lee and S. Yoshida, *Astrophys. J.* **586**, 403 (2003), astro-ph/0211580.
- [46] N. Andersson, K. Glampedakis, and B. Haskell, *Phys. Rev. D* **79**, 103009 (2009), 0812.3023.
- [47] H. Heiselberg and M. Hjorth-Jensen, *Astrophys. J. Lett.* **525**, L45 (1999), astro-ph/9904214.
- [48] A. Akmal, V. R. Pandharipande, and D. G. Ravenhall, *Phys. Rev. C* **58**, 1804 (1998).
- [49] S. Goriely, N. Chamel, and J. M. Pearson, *Phys. Rev. C* **88**, 024308 (2013).
- [50] J. M. Pearson, N. Chamel, A. Y. Potekhin, A. F. Fantina, C. Ducoin, A. K. Dutta, and S. Goriely, *Mon. Not. R. Astron. Soc.* **481**, 2994 (2018), 1903.04981.
- [51] M. E. Gusakov, A. D. Kaminker, D. G. Yakovlev, and O. Y. Gnedin, *Mon. Not. R. Astron. Soc.* **363**, 555 (2005), astro-ph/0507560.
- [52] P. S. Shternin, D. G. Yakovlev, C. O. Heinke, W. C. G. Ho, and D. J. Patnaude, *MNRAS* **412**, L108 (2011).
- [53] D. Page, M. Prakash, J. M. Lattimer, and A. W. Steiner, *Phys. Rev. Lett.* **106**, 081101 (2011).
- [54] K. G. Elshamouty, C. O. Heinke, G. R. Sivakoff, W. C. G. Ho, P. S. Shternin, D. G. Yakovlev, D. J. Patnaude, and L. David, *Astrophys. J.* **777**, 22 (2013), 1306.3387.
- [55] W. C. G. Ho, K. G. Elshamouty, C. O. Heinke, and A. Y. Potekhin, *Phys. Rev. C* **91**, 015806 (2015), 1412.7759.

- [56] S. Beloin, S. Han, A. W. Steiner, and D. Page, Phys. Rev. C **97**, 015804 (2018).
- [57] A. Gezerlis, C. J. Pethick, and A. Schwenk, ArXiv e-prints (2014), 1406.6109.
- [58] J. M. Dong, U. Lombardo, and W. Zuo, Physics of Atomic Nuclei **77**, 1057 (2014).
- [59] D. Ding, A. Rios, H. Dussan, W. H. Dickhoff, S. J. Witte, A. Carbone, and A. Polls, Phys. Rev. C **94**, 025802 (2016), URL <https://link.aps.org/doi/10.1103/PhysRevC.94.025802>.
- [60] A. Sedrakian and J. W. Clark, European Physical Journal A **55**, 167 (2019), 1802.00017.
- [61] A. S. Parikh and R. Wijnands, Mon. Not. R. Astron. Soc. **472**, 2742 (2017), 1707.05606.
- [62] M. E. Gusakov, E. M. Kantor, A. I. Chugunov, and L. Gualtieri, Mon. Not. R. Astron. Soc. **428**, 1518 (2013), 1211.2452.
- [63] F. Özel, D. Psaltis, R. Narayan, and A. Santos Villarreal, Astrophys. J. **757**, 55 (2012), 1201.1006.
- [64] J. Antoniadis, T. M. Tauris, F. Özel, E. Barr, D. J. Champion, and P. C. C. Freire, arXiv e-prints arXiv:1605.01665 (2016), 1605.01665.
- [65] M. Oertel, M. Hempel, T. Klähn, and S. Typel, Reviews of Modern Physics **89**, 015007 (2017), 1610.03361.
- [66] G. Fiorella Burgio and A. F. Fantina, *Nuclear Equation of State for Compact Stars and Supernovae* (2018), vol. 457 of *Astrophysics and Space Science Library*, p. 255.
- [67] L. Bildsten and G. Ushomirsky, Astrophys. J. Lett. **529**, L33 (2000), astro-ph/9911155.
- [68] Y. Levin and G. Ushomirsky, Mon. Not. R. Astron. Soc. **324**, 917 (2001), astro-ph/0006028.
- [69] K. Glampedakis and N. Andersson, Phys. Rev. D **74**, 044040 (2006), astro-ph/0411750.
- [70] M. Nayyar and B. J. Owen, Phys. Rev. D **73**, 084001 (2006), astro-ph/0512041.
- [71] M. G. Alford, S. Mahmoodifar, and K. Schwenzer, Phys. Rev. D **85**, 024007 (2012), 1012.4883.
- [72] D. D. Ofengeim, M. E. Gusakov, P. Haensel, and M. Fortin, Phys. Rev. D **100**, 103017 (2019), 1911.08407.
- [73] B. Haskell, N. Andersson, and A. Passamonti, Mon. Not. R. Astron. Soc. **397**, 1464 (2009), 0902.1149.